

Referee #3

In their work, Xu et al. develop two new tree-rings isotopic chronologies of $\delta^{18}\text{O}$ from Northern India, and, combined with three other $\delta^{18}\text{O}$ chronologies, propose a multi-decadal regional reconstruction of the Indian summer monsoon. The regional record is further investigated using correlation and spectral analyses to document: 1) the drivers of Indian summer monsoon variability, and 2) the long-term trends of Indian summer monsoon intensity.

The new Data and this regional reconstruction are valuable to document a key hydroclimate component of the region, which lacks high resolution and long-term proxy records.

The methodology used in this paper as well as the results are robust. The data analyses, however, would benefit from further in depth exploration of each chronology signal. The discussion needs more regional scope but this can be improved if more data analyses are carried.

General Comments

- The authors present only correlations between the five $\delta^{18}\text{O}$ chronologies. How are the correlations for high and low frequency between the 5 chronologies?

Answer: Thanks for your helpful suggestions. We have added the correlation coefficient between the five $\delta^{18}\text{O}$ chronologies at multi-decadal time scale into Table 2 and the related sentences “the five tree ring $\delta^{18}\text{O}$ records for the Himalaya region are significantly correlated with each other at inter-annual time scale during the common period, and in most cases 31-year running averages of five tree ring $\delta^{18}\text{O}$ chronologies show significant correlations at multi-decadal time scale (Table 2)” in the manuscript. In general, the correlation coefficient among $\delta^{18}\text{O}$ chronologies decreased when the distances between two near $\delta^{18}\text{O}$ chronologies increased.

Table 2: Correlation coefficients between the tree ring $\delta^{18}\text{O}$ records from different sampling locations.

<i>r</i> -annual	Manali	JG	Hulma	Ganesh
JG	0.50*			
Hulma	0.52*	0.51*		
Ganesh	0.47*	0.66*	0.61*	
Wache	0.23*	0.26*	0.37*	0.52*

<i>r</i> -multi-decadal	Manali	JG	Hulma	Ganesh
JG	0.36*			
Hulma	0.37*	0.64*		
Ganesh	-0.03	0.94*	0.66*	
Wache	0.11	0.39*	0.38*	0.70*

* $p < 0.01$

- Climate correlations for each chronology $\delta^{18}\text{O}$ are summarized in the text however a figure of correlation between each chronology and the main climate factor (precipitation and/or PDSI) should be presented to assess the climate signal in each chronology before creating the composite regional signal.

Answer: Thanks for your helpful suggestion. We have added the correlation between tree ring $\delta^{18}\text{O}$ in five sites and regional June-September PDSI/Precipitation in Table 1. Because the correlations between tree ring $\delta^{18}\text{O}$ in Manali, Hulma and Wache and monsoon season (JJAS) precipitation/PDSI were already showed and mechanisms that JJAS precipitation/PDSI affect tree ring $\delta^{18}\text{O}$ in Manali, Hulma and Wache were already explained in previous study. (Sano et al., 2011, 2013, and submitted), we added climatic response of each tree ring $\delta^{18}\text{O}$ chronology in Table 1.

Table 1. Tree ring cellulose oxygen isotope data sets used in this study

No.	Sample ID	Location	Period	Tree species	Mean (1951-2000)	Climatic response of tree ring $\delta^{18}\text{O}$	Data source
1	Manali	32°13'N, 77°13'E, 2700 masl, India	1768-2008	<i>Abies pindrow</i>	29.97‰	Regional JJAS PDSI $r = -0.67$	Sano et al., submitted
2	JG	29°38'N, 79°51'E, 3849 masl, India	1641-2008	<i>Cedrus deodara</i>	30.39‰	Regional JJAS PDSI $r = -0.50$	This study
3	Hulma	29°51'N, 81°56'E, 3850 masl, Nepal	1778-2000	<i>Abies spectabilis</i>	25.94‰	Regional JJAS PDSI $r = -0.73$	Sano et al., 2011
4	Ganesh	28°10'N, 85°11'E, 3550 masl, Nepal	1801-2000	<i>Abies spectabilis</i>	23.01‰	Regional JJAS PDSI $r = -0.55$	This study
5	Wache	27°59'N, 90°00'E, 3500 masl, Bhutan	1743-2011	<i>Larix griffithii</i>	19.38‰	Regional JJAS Precipitation $r = -0.59$	Sano et al., 2013

- The composite signal (average of 5 centered $\delta^{18}\text{O}$ chronologies) should be presented with a standard deviation or an uncertainty term in order to see if the uncertainty changed over time. This will be important to discuss the relationship between the composite regional signal and its relation with Indian summer monsoon indices for the last ~200 years.

Answer: Thanks for your helpful suggestion. We have added the 95% ($\pm 1.96\sigma$) confidence limits to evaluate the uncertainty not only for the regional chronology but also for each tree ring $\delta^{18}\text{O}$ chronology (except for chronology in Hulma, because the tree ring oxygen isotopes chronology was produced by pooling method, and therefore the uncertainty of this chronology was not able to show). Please see the following figure. gray shadows show the 95% ($\pm 1.96\sigma$) confidence limits for each chronology.

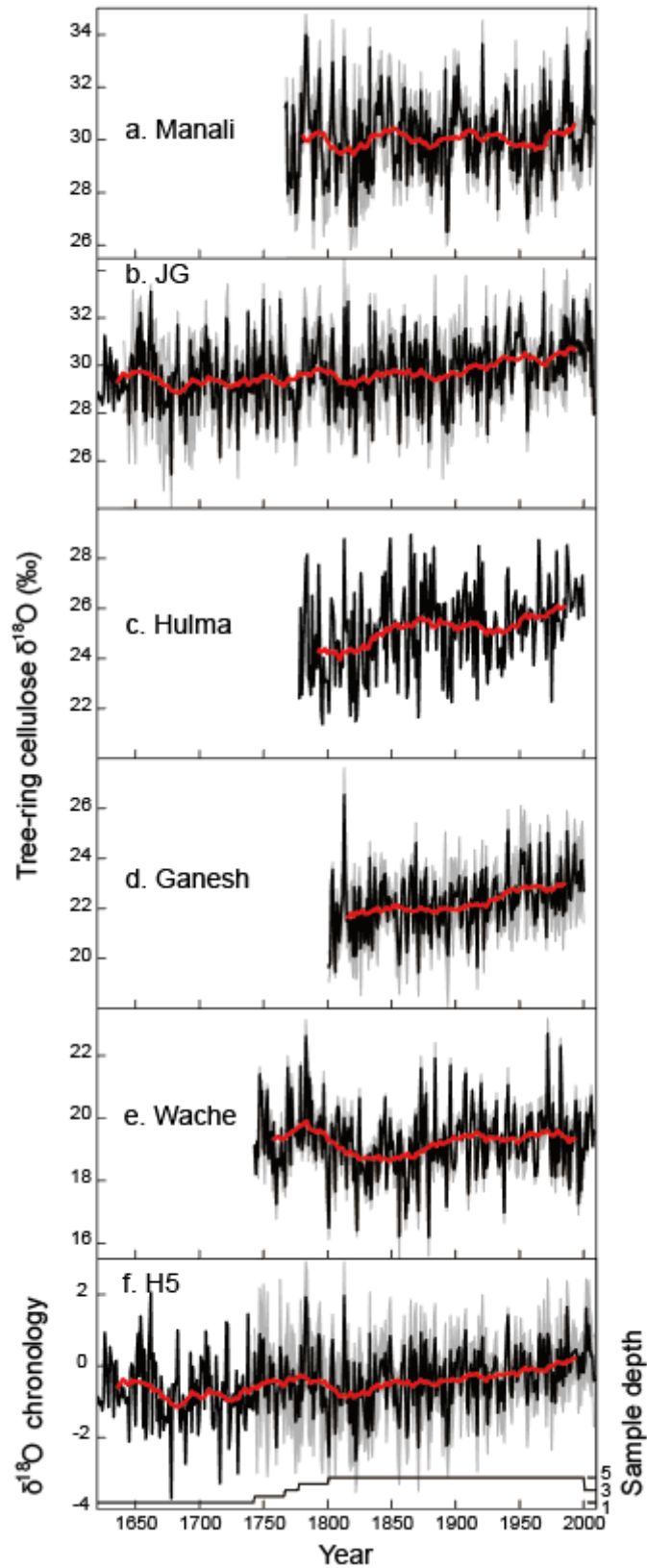


Figure Caption: New Figure 4: Tree ring oxygen isotope chronologies from five sites (a-e) and the regional tree ring oxygen isotope chronology (f). (black line: mean values for all samples; red line: 31-year running average for the chronology; gray shadows: the 95% ($\pm 1.96\sigma$) confidence limits)

- The $\delta^{18}\text{O}$ signal is often described from a theoretical perspective. Could the authors provide more evidence of the $\delta^{18}\text{O}$ signal in these particular chronologies? Comparison with RH or source water isotopes? Or using process based evaluation by means of $\delta^{18}\text{O}$ forward modelling (Eg. Evans 2007).

Answer: Source water $\delta^{18}\text{O}$ and relative humidity are two main controlling factor for tree ring cellulose $\delta^{18}\text{O}$. Comparison between tree ring $\delta^{18}\text{O}$ and source water $\delta^{18}\text{O}$ /relative humidity and using tree ring $\delta^{18}\text{O}$ forward modelling would be helpful to understand source water $\delta^{18}\text{O}$ and relative humidity influences' on tree ring $\delta^{18}\text{O}$. However, long-term continuous precipitation $\delta^{18}\text{O}$ records are scarce in the study area. A better model parameterization for each species in each site depends on many observed parameters that are not available in five sites. The good things are that previous studies already showed the relationship between precipitation $\delta^{18}\text{O}$ /relative humidity and tree ring $\delta^{18}\text{O}$ in study area. For example, Sano et al. (2011) indicated that tree ring $\delta^{18}\text{O}$ in Hulma showed negative correlations with June-September relative humidity and positive correlations with June-September precipitation $\delta^{18}\text{O}$ in New Delhi. Sano et al., (submitted) revealed that tree ring $\delta^{18}\text{O}$ in Manali showed the negative correlations with June-September relative humidity. In some sites, relative humidity record is not available. PDSI was employed to evaluate the relationship between tree ring $\delta^{18}\text{O}$ and moisture condition. Tree ring $\delta^{18}\text{O}$ in JG, Ganesh and Wache showed negative correlations with regional PDSI. Such negative correlations between tree ring $\delta^{18}\text{O}$ and summer PDSI or relative humidity have also been found in other areas of monsoonal Asia, such as northern Laos (Xu et al., 2013a), northern Vietnam (Sano et al., 2012), southeast Tibet Plateau (Grießinger et al., 2011; 2016, Liu et al., 2013, Wernicke et al., 2015), southeast China (Xu et al., 2013b, Xu et al., 2016) and Japan (Sakashita et al., 2015; Yamaguchi et al., 2010).

- Grießinger J, Bräuning A, Helle G, Thomas A, Schleser G (2011) Late Holocene Asian summer monsoon variability reflected by $\delta^{18}\text{O}$ in tree-rings from Tibetan junipers. *Geophysical Research Letters* 38 (3):L03701
- Grießinger J, Bräuning A, Helle G, Hochreuther P, Schleser G (2016) Late Holocene relative humidity history on the southeastern Tibetan plateau inferred from a tree-ring $\delta^{18}\text{O}$ record: Recent decrease and conditions during the last 1500 years. *Quaternary International*, In press
- Liu X, Zeng X, Leavitt SW, Wang W, An W, Xu G, Sun W, Yu W, Qin D, Ren J (2013) A 400-year tree-ring $\delta^{18}\text{O}$ chronology for the southeastern Tibetan Plateau: Implications for inferring variations of the regional hydroclimate. *Global & Planetary Change* 104:23-33
- Sakashita W, Yokoyama Y, Miyahara H, (2015) Relationship between early summer precipitation in Japan and the El Niño-Southern and Pacific Decadal Oscillations over the past 400 years. *Quaternary International*, 397(4):300-306.
- Sano M, Xu C, Nakatsuka T (2012). A 300-year Vietnam hydroclimate and ENSO variability record reconstructed from tree ring $\delta^{18}\text{O}$. *Journal of Geophysical Research Atmospheres*, 117(D12):12115.
- Wernicke J, Grießinger J, Hochreuther P, Bräuning A (2015) Variability of summer humidity during the past 800 years on the eastern Tibetan Plateau inferred from $\delta^{18}\text{O}$ of tree-ring cellulose. *Climate of the Past* 11:327-337
- Xu C, Sano M, Nakatsuka T(2013a). A 400-year record of hydroclimate variability and local ENSO history in northern Southeast Asia inferred from tree-ring $\delta^{18}\text{O}$.

Palaeogeography Palaeoclimatology Palaeoecology, 386:588-598.

Xu C, Zheng H, Nakatsuka T, Sano M (2013b) Oxygen isotope signatures preserved in tree ring cellulose as a proxy for April–September precipitation in Fujian, the subtropical region of southeast China. *Journal of Geophysical Research: Atmospheres* 118 (23):12,805-812,815

Xu C., J. Ge, T. Nakatsuka, L. Yi, H. Zheng, and M. Sano (2016), Potential utility of tree ring $\delta^{18}\text{O}$ series for reconstructing precipitation records from the lower reaches of the Yangtze River, southeast China, *J. Geophys. Res. Atmos.*, 121, doi:10.1002/2015JD023610.

Yamaguchi Y T, Hughen K A. (2010) Synchronized Northern Hemisphere climate change and solar magnetic cycles during the Maunder Minimum. *Proceedings of the National Academy of Sciences of the United States of America*, 107(48):20697-20702.

- Analyses of observations would enhance the strength of the tree rings data: trends of rainfall for the region, as well as the various indices discussed in the paper. Additionally, $\delta^{18}\text{O}$ tree-rings and rainfall amount over the observations period should be plotted to strengthen the interpretation of the amount effect described in the results-discussion sections. This can be done for each site or at regional scale.

Answer: Thanks for your suggestion. We have added the description of nature of long-term variations in modern instrumental rainfall data based on the Sontakke et al., 2008 and Bhutiyani et al., 2010 in section 3.4 (*Centennial variability of the ISM inferred from the regional tree ring $\delta^{18}\text{O}$ record*). Please see the Section 3.4 (below).

Sontakke, N. A., Singh, N., and Singh, H. N.: Instrumental period rainfall series of the Indian region (AD1813-2005): revised reconstruction, update and analysis, *Holocene*, 18(7), 1055-1066, 2008.

Bhutiyani, M. R., Kale, V. S., and Pawar, N J: Climate change and the precipitation variations in the northwestern Himalaya: 1866-2006, *International Journal of Climatology*, 30(4), 535-548, 2010.

On the amount effect, we employed the amount effect to explain that how ISM affect tree ring $\delta^{18}\text{O}$. At regional scales, regional tree ring $\delta^{18}\text{O}$ show significant negative correlations with June-September precipitation in northern India. The following figure supports the amount effect to some extent.

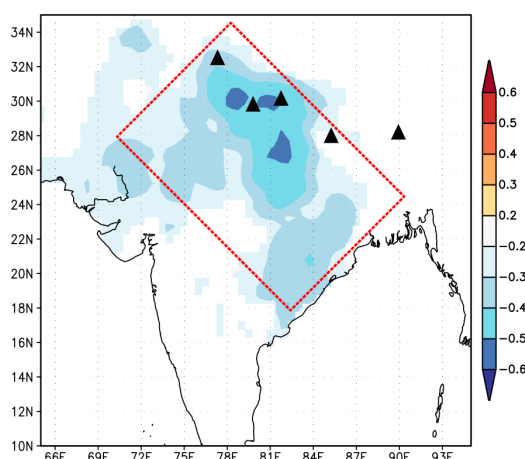


Figure 6. Spatial correlations between the H5 regional tree ring $\delta^{18}\text{O}$ record with June-September precipitation from GPCP V7 over interval from 1901-2008 CE. Only correlations significant at the 95% level are shown.

3.4 Centennial variability of the ISM inferred from the regional tree ring $\delta^{18}\text{O}$ record

There are also significant centennial-scale variations in the H5 record (Figure 7), which were extracted using a 100-year low-pass filter (Figure 10c, red line). The record exhibits a decreasing trend from 1743 to 1820 CE and an increasing trend since 1820 CE, which indicates a weakening trend of the ISM during the interval from 1820-2000 CE. A reduction in the monsoon precipitation/relative humidity of the ISM in the last 200 years is also evident in other areas influenced by the ISM. Maar lake sediments in Myanmar exhibit a decreasing trend of monsoonal rainfall since 1840 CE (Sun et al., 2016); a tree ring $\delta^{18}\text{O}$ record from southeast Asia exhibits a drying trend since 1800 CE (Xu et al., 2013a); a stalagmite $\delta^{18}\text{O}$ record from southwest China reveals an overall decreasing trend in monsoon precipitation since 1760 CE (Tan et al., 2016); and in southwest China, tree ring $\delta^{18}\text{O}$ and maar lake records indicate reduced monsoon precipitation/relative humidity/cloud cover since 1840 or 1860 CE (Chu et al., 2011; Griebinger et al., 2016; Liu et al., 2014; Wernicke et al., 2015; Xu et al., 2012). **Monsoon precipitation in northwestern India shows a significant decreasing trend during the period of 1866-2006 (Bhutiyan et al., 2010).**

However, in contrast, marine sediment records from the Western and Southeastern Arabian Sea exhibit an increasing trend of ISM strength over the last four centuries (Anderson et al., 2002; Chauhan et al., 2010). A recent study indicated that the contrasting trends in the ISM during the last several hundred years observed in geological records resulted from the different behavior of the Bay of Bengal branch and Arabian Sea branch of the ISM (Tan et al., 2016), **and the Bay of Bengal branch of ISM weakened while intensity of Arabian Sea branch of the ISM increased during the last 200 years. However, the tree ring $\delta^{18}\text{O}$ record in northwest India, influenced by the Arabian Sea branch of the ISM, exhibits a drying trend since 1950 CE (Sano et al., submitted), which does not support the idea of a strengthening Arabian Sea branch of the ISM (Anderson et al., 2002).** Moreover, there are no calibrated radiocarbon dates for the last 300 years for the two records from the Arabian Sea (Anderson et al., 2002a; Chauhan et al., 2010). We suggest that further high-resolution and well-dated ISM records from western India are needed to improve our understanding of the behavior of the ISM. **Although reconstructed All India monsoon rainfall does not show a significant decreasing trend during the period of 1813-2005 (Sontakke et al., 2008), the data from only four stations extend back to 1826 CE and four longest stations locate in central or southern India. Monsoon season drying trend in northern India revealed by H5 regional tree ring $\delta^{18}\text{O}$ record may indicate that inland areas appear to be particularly sensitive to the weakening of monsoon circulation.**

The H5 record suggests a decreasing trend of ISM strength, which is supported by most of the other well-dated and high-resolution ISM records in ISM margin areas. A previous study has indicated that solar irradiance has a significant influence on the ISM on multi-decadal to centennial timescales, and that reduced solar output is correlated with weaker ISM winds (Gupta et al., 2005). However, solar irradiance has increased

since 1810-1820 CE (Bard et al., 2000; Lean et al., 1995) and therefore it cannot be the main reason for the weaker ISM since 1820 CE. Atmospheric CO₂ content is another forcing factor for the ISM, with higher atmospheric CO₂ content resulting in a stronger ISM (Kripalani et al., 2007; Meehl and Washington, 1993). Thus, the increased atmospheric CO₂ content during the last 200 years is unlikely to be the reason for the weakened ISM.

The land-sea thermal contrast which is also an important influencing factor for ISM (Roxy et al., 2015), is evaluated by atmospheric temperature gradient between the Tibetan Plateau and the tropical Indian Ocean (Fu and Fletcher, 1985; Sun et al., 2010). The history of land-sea thermal contrasts is reconstructed based on temperature differences between the Tibetan Plateau and the Indian Ocean (Figure 10a), and centennial variations of land-sea thermal contrasts are shown in Figure 10b. Three reconstructed land-sea thermal contrasts showed a decreasing trend since 1800 CE and 1820 CE (Figure 10b), and the H5 record exhibits a similar pattern of changes on a centennial scale (Figure 10c). The decreasing land-sea thermal contrast since 1800 and 1820 CE has resulted in a weaker ISM, and the increasing trend of the H5 record since 1820 CE also indicates a reduced ISM intensity. In addition, aerosol emissions may be another reason to cause weakened ISM. Because the aerosol-induced differential cooling of the source and nonsource regions resulted in not only reduced local land-ocean surface thermal contrast but also weaken large-scale meridional atmospheric temperature gradients, both of which caused weakening Indian summer monsoon circulation (Bollasina et al., 2011; Cowan and Cai, 2011). Long-term aerosol emissions record is needed to evaluate aerosol emission's influences on ISM in the past.

- In Page 9 paragraph 1 (~ line 5): Is the RH threshold 1%?

Answer: Yes, we refer to the results from Managave (2014). Maybe our explanation on relative humidity's influence on the correlation between two proxies is not so clear. We have revised this part. "Relative humidity has an important impact on tree ring $\delta^{18}\text{O}$ (Roden et al., 2000). Lower relative humidity result in enhanced evaporative enrichment of leaf water and then higher tree ring cellulose $\delta^{18}\text{O}$, while the relative humidity may not affect speleothem $\delta^{18}\text{O}$ when relative humidity does not correlate with precipitation $\delta^{18}\text{O}$ (Managave, 2014). Model results show that relative humidity's influences on the correlation between tree ring $\delta^{18}\text{O}$ and speleothem $\delta^{18}\text{O}$ is more pronounced in the regions where the variation of relative humidity during the growing season exceeds 1% (Managave, 2014)."

Managave, S. R.: Model evaluation of the coherence of a common source water oxygen isotopic signal recorded by tree-ring cellulose and speleothem calcite, *Geochemistry Geophysics Geosystems*, 15, 905–922, 2014.

- In Page 9 paragraph 1 (~ line 5): further discussion is required when assessing how the source $\delta^{18}\text{O}$ is integrated differently between tree-rings and speleothem proxies.

Answer: Thanks for your helpful suggestion. We have revised this part. Please see the revised part. "Based on the oxygen isotope fractionation theory, tree ring $\delta^{18}\text{O}$ and speleothem $\delta^{18}\text{O}$ should share similar changes (Managave, 2014) if both of them inherit a common source water $\delta^{18}\text{O}$ signal, as shown by Ramesh, et al (2013). The following reasons may cause incoherence between regional tree ring $\delta^{18}\text{O}$ and speleothem $\delta^{18}\text{O}$.

Other controlling factors differentially affect tree ring $\delta^{18}\text{O}$ and speleothem $\delta^{18}\text{O}$ values. Relative humidity has an important impact on tree ring $\delta^{18}\text{O}$ (Roden et al., 2000). Lower relative humidity result in enhanced evaporative enrichment of leaf water and then higher tree ring cellulose $\delta^{18}\text{O}$, while the relative humidity may not affect speleothem $\delta^{18}\text{O}$ when relative humidity does not correlate with precipitation $\delta^{18}\text{O}$ (Managave, 2014). Model results show that relative humidity's influences on the correlation between tree ring $\delta^{18}\text{O}$ and speleothem $\delta^{18}\text{O}$ is more pronounced in the regions where the variation of relative humidity during the growing season exceeds 1% (Managave, 2014). In contrast, the cave epikarst dynamics affect speleothems $\delta^{18}\text{O}$ significantly (Lachniet, 2009). The infiltrating water from different rainfall events may be stored and mixed in the epikarst. Lag times of $\delta^{18}\text{O}$ values in drip waters relative to rainfall are several years or decades in some locations (Lachniet, 2009), and a slow transit time smoothed climate signal. These processes may result in different source water for tree ring and speleothem. In addition, limited three ^{230}Th dates points (3 control points) and relative large age uncertainty (9-31 years) of speleothems $\delta^{18}\text{O}$ time series during the common period of 1743-2000 may result in the incoherence between tree ring and speleothems $\delta^{18}\text{O}$. Long-term process-based study on tree ring $\delta^{18}\text{O}$ and speleothem $\delta^{18}\text{O}$ variations in future study are needed for a better understanding for climatic implication of two proxies.”

- Page 10 from line 10 to 25: the text needs substantial editing, there are lot of repetitions and the discussion is not clear. Often the authors start describing the implication of their record and its comparison with regional records without an in-depth discussion.

Answer: Thanks for your helpful suggestion. We have described the implication of our records and comparison with other records in the study in previous paragraphs. In this paragraph, we try to explain the reason that caused the weakened ISM. We revised this paragraph. Please see the revised part. “The land-sea thermal contrast which is also an important influencing factor for ISM (Roxy et al., 2015), is evaluated by atmospheric temperature gradient between the Tibetan Plateau and the tropical Indian Ocean (Fu and Fletcher, 1985; Sun et al., 2010). The history of land-sea thermal contrasts is reconstructed based on temperature differences between the Tibetan Plateau and the Indian Ocean (Figure 10a), and centennial variations of land-sea thermal contrasts are shown in Figure 10b. Three reconstructed land-sea thermal contrasts showed a decreasing trend since 1800 CE and 1820 CE (Figure 10b), and the H5 record exhibits a similar pattern of changes on a centennial scale (Figure 10c). The decreasing land-sea thermal contrast since 1800 and 1820 CE has resulted in a weaker ISM, and the increasing trend of the H5 record since 1820 CE also indicates a reduced ISM intensity. In addition, aerosol emissions may be another reason to cause weakened ISM. Because the aerosol-induced differential cooling of the source and nonsource regions resulted in not only reduced local land-ocean surface thermal contrast but also weaken large-scale meridional atmospheric temperature gradients, both of which caused weakening Indian summer monsoon circulation (Bollasina et al., 2011; Cowan and Cai, 2011). Long-term aerosol emissions record is needed to evaluate aerosol emission's influences on ISM in the past.”

- Page 9 starting line ~20. The discussion here is interesting, however, needs some clarification and editing.

Answer: Thanks for your helpful suggestion. We have revised this paragraph according

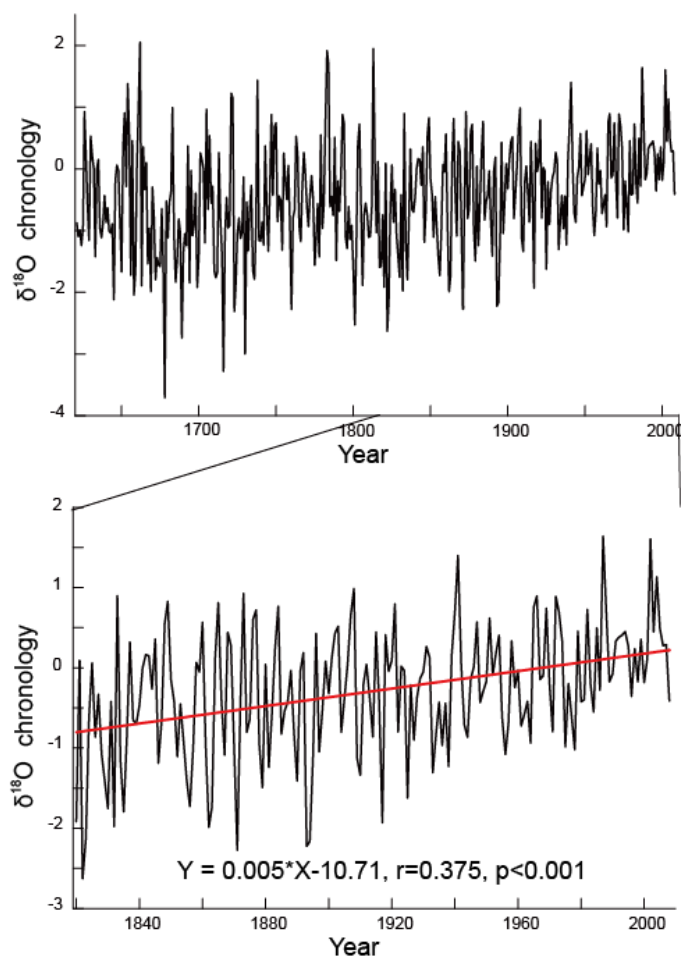
to your suggestion. Please see the revised part. “However, in contrast, marine sediment records from the Western and Southeastern Arabian Sea exhibit an increasing trend of ISM strength over the last four centuries (Anderson et al., 2002; Chauhan et al., 2010). A recent study indicated that the contrasting trends in the ISM during the last several hundred years observed in geological records resulted from the different behavior of the Bay of Bengal branch and Arabian Sea branch of the ISM (Tan et al., 2016), and the Bay of Bengal branch of ISM weakened while intensity of Arabian Sea branch of the ISM increased during the last 200 years. However, the tree ring $\delta^{18}\text{O}$ record in northwest India, influenced by the Arabian Sea branch of the ISM, exhibits a drying trend since 1950 CE (Sano et al., submitted), which does not support the idea of a strengthening Arabian Sea branch of the ISM (Anderson et al., 2002). Moreover, there are no calibrated radiocarbon dates for the last 300 years for the two records from the Arabian Sea (Anderson et al., 2002a; Chauhan et al., 2010). We suggest that further high-resolution and well-dated ISM records from western India are needed to improve our understanding of the behavior of the ISM. Although reconstructed All India monsoon rainfall does not show a significant decreasing trend during the period of 1813-2005 (Sontakke et al., 2008), the data from only four stations extend back to 1826 CE and four longest stations locate in central or southern India. Monsoon season drying trend in northern India revealed by H5 regional tree ring $\delta^{18}\text{O}$ record may indicate that inland areas appear to be particularly sensitive to the weakening of monsoon circulation.”

For the clarification: 1) the authors report a decreasing $\delta^{18}\text{O}$ trend from 1743-1820. How many chronologies are included in this part of the record? According to Table 1 and Figure 4, only 2 chronologies extend back to 1743. Authors should use caution when making regional trend interpretations

Answer: Thanks for your helpful suggestion. We have added the sample depth in Figure. Please see the revised Figure 4 in Page 3 of this file. There are three tree ring $\delta^{18}\text{O}$ chronologies since 1767 CE. The main conclusion is based on the result since 1800 CE. There are five tree ring $\delta^{18}\text{O}$ chronologies since 1800 CE.

2) an increasing $\delta^{18}\text{O}$ trend from 1820 to 2000 is observed in the $\delta^{18}\text{O}$ tree-rings interpreted as an increase in the Indian monsoon intensity, also observed from other regional proxies. Is this trend also observed when considering the chronologies individually? What are the statistics for this trend?

Answer: an increasing tree ring $\delta^{18}\text{O}$ trend from 1820 to 2000 is interpreted as a decrease in the Indian monsoon intensity. Such increasing trend of tree ring $\delta^{18}\text{O}$ from 1820 to 2000 is also found in JG, Hulma, Ganesh and Wache (Please see Figure in Page in this file). The increased trend of regional tree ring $\delta^{18}\text{O}$ chronology during the period of 1820-2008 was tested using linear regression. Please see the following figure and Figure in Page 11 in this file.



- Page 10, line 20. The discussion of factors (for instance aerosols) other than the decreasing land-ocean thermal contrast and their role in the decreasing Indian Monsoon intensity needs to be more detailed. What is the land-ocean thermal contrast resolution, interannual? Decadal? From Figure 11 the proxy records for ocean and land temperature do not seem to have the same temporal resolution.

Answer: Thanks for your suggestion. We have added the sentences on how the aerosols affect Indian summer monsoon. Please see the following paragraph. “Because the aerosol-induced differential cooling of the source and nonsource regions resulted in not only reduced local land-ocean surface thermal contrast but also weaken large-scale meridional atmospheric temperature gradients, both of which caused weakening Indian summer monsoon circulation (Bollasina et al., 2011; Cowan and Cai, 2011).”

For the land-ocean thermal contrast, temperature reconstruction in Tibet Plateau (Shi et al., 2015) represents a 10-year moving average and the resolution of SST reconstruction is annual in previous manuscript. In revised manuscript, we have added two annual-resolution summer temperature reconstruction in Tibetan Plateau (Cook et al., 2013; Wang et al., 2015) to evaluate the land-ocean thermal contrast history. Please see the following figure.

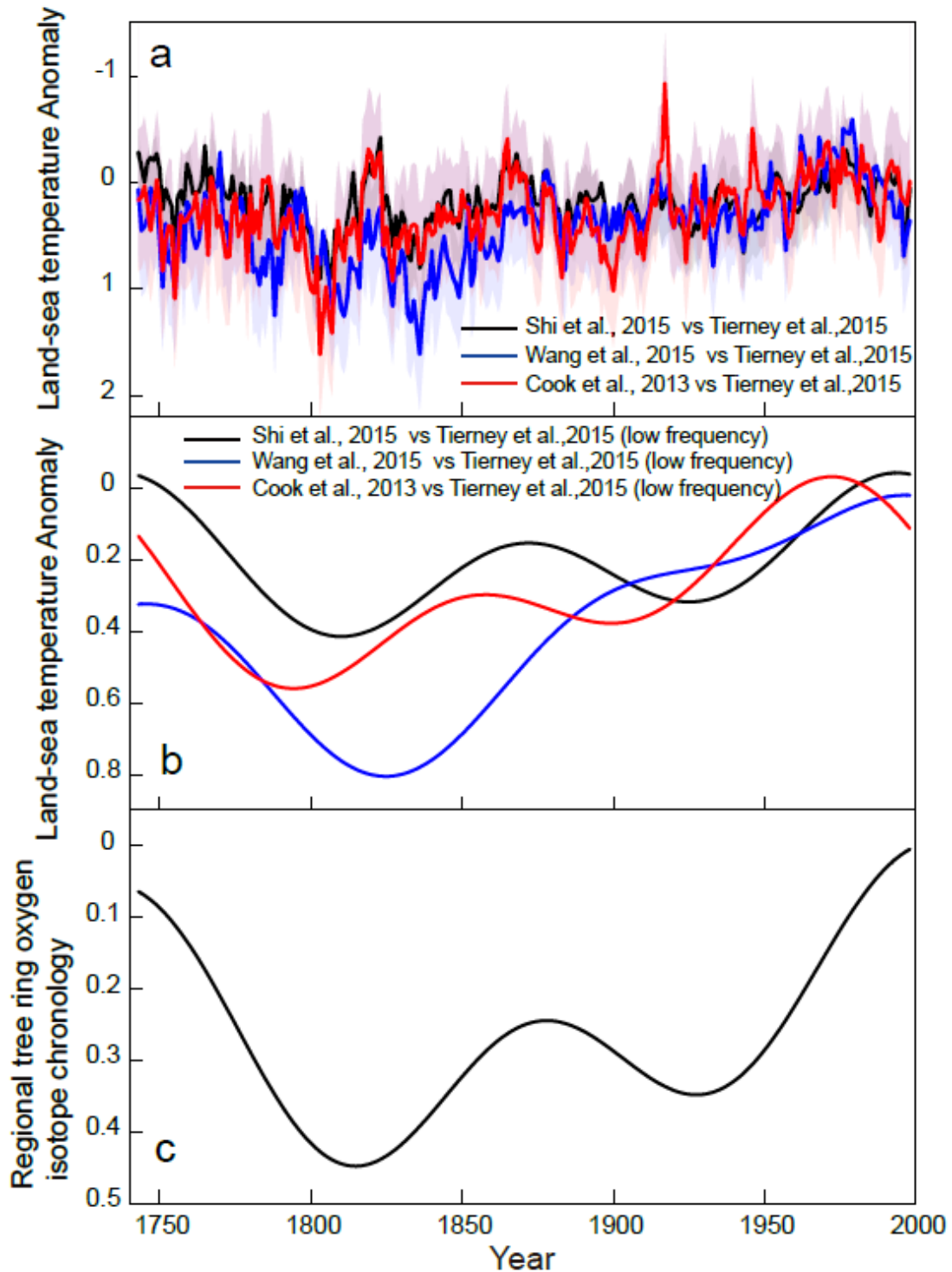


Figure Caption: Figure 10. a: Land-sea Temperature Anomaly based on three summer temperature reconstruction for the Tibetan Plateau and one Indian Ocean SST reconstruction; b and c: centennial variations of land-sea thermal contrasts and the H5 regional tree ring $\delta^{18}\text{O}$ chronology.

- when assessing the ENSO-and H5 regional $\delta^{18}\text{O}$ correlations, a 31-year window is too large (ENSO is 2-7 years). It would be helpful to investigate ENSO- and Tree-rings $\delta^{18}\text{O}$ correlation for individual chronologies to test whether the decorrelation is observed for all chronologies which reflect sites under slightly different precipitation

regime and Indian summer monsoon influence (based on Fig 1).

Answer: ENSO-Monsoon teleconnection is known to be a nonstationary process. We need to evaluate how the relationships between ENSO and monsoon changed in the past. Because ENSO has the strongest power in wave length or cycles 2-7 yr, 31-year or 21-year window moving correlations between ENSO and precipitation were used to evaluate the stability of relationship between ENSO and climate. The 31-year and 21-year window can cover the main cycles (2-7 years) of ENSO. For example, Camberlin et al., (2004, *Climate Dynamics*) used 31-year moving correlations between NINO3 SST and seasonal rainfall anomalies over a few regions to see ENSO/rainfall teleconnections. 21-year moving window correlation analysis between ENSO and climate was used to investigate the relationship between ENSO and East Asian winter monsoon/precipitation and flood pulse in the Mekong River Basin (Kim et al., 2016; Räsänen and Kummu, 2013)

Thanks for your helpful suggestion on the relationship between individual tree ring $\delta^{18}\text{O}$ chronology and ENSO. We did not add the related part in previous manuscript based on two reasons. 1) this manuscript mainly focused on the variations of ISM at regional scale rather than local scale. 2) Due to the complexity of ENSO-monsoon relationship, more tree ring $\delta^{18}\text{O}$ chronologies from Asian monsoon area (for example, Laos, Myanmar, Thailand, Vietnam, China and Japan) are needed. Now we are working on ENSO-Asian summer monsoon relationship based on lots of tree ring chronologies from Asian monsoon area.

Camberlin P, Chauvin F, Douville H, et al. Simulated ENSO-tropical rainfall teleconnections in present-day and under enhanced greenhouse gases conditions. *Climate Dynamics*, 2004, 23(6):641-657.

Kim J W, An S I, Jun S Y, et al. ENSO and East Asian winter monsoon relationship modulation associated with the anomalous northwest Pacific anticyclone. *Climate Dynamics*, 2016:1-23.

Räsänen T A, Kummu M. Spatiotemporal influences of ENSO on precipitation and flood pulse in the Mekong River Basin. *Journal of Hydrology*, 2013, 476(1):154-168.

Specific comments

- In Results and Discussion, section 3.1. The standard deviation of individual tree-ring cores can be added next to the mean.

Answer: Thanks for your suggestion. We have modified the section 3.1 according to your suggestion. Please see the revised part. “The oxygen isotopes of four individuals of *Abies spectabilis* in Ganesh (GE, central Nepal) and three individuals of *Cedrus deodara* in Jageshwar (JG, northern India) were measured for the interval from 1801-2000 CE and 1643-2008 CE, respectively. Individual tree ring $\delta^{18}\text{O}$ time series from four cores from central Nepal are shown in Figure 2a. The mean values (standard deviations) of the $\delta^{18}\text{O}$ time series from 224c, 233b, 235b, and 226a are 23.09‰(1.22‰), 22.66‰(1.27‰), 21.87‰(1.12‰), and 22.94‰(1.42‰), respectively, from 1901-2000 CE. The inter-tree differences in $\delta^{18}\text{O}$ values are small. The $\delta^{18}\text{O}$ values of the four cores exhibit peaks in 1813. The mean inter-series correlations (R_{bar}) among the cores range from 0.56-0.78 (Figure 2c), based on a 50-year window over the interval from 1801-2000 CE.

Three tree ring $\delta^{18}\text{O}$ time series from northern India (JG) are shown in Figure 3a. The mean values (standard deviations) of the $\delta^{18}\text{O}$ time series from 101c, 102c, and 103a are 30.11‰(1.49‰), 29.7‰(1.62‰) and 29.47‰(1.53‰), respectively, over the interval from 1694-2008 CE. Three tree ring $\delta^{18}\text{O}$ time series in JG exhibit a consistent pattern of variations. The mean inter-series correlations (R_{bar}) among the cores range from 0.61-0.78 (Figure 3c), based on a 50-year window over the interval from 1641-2008 CE.”

- In Table 1 the mean $\delta^{18}\text{O}$ for each chronology should have a unit (‰)

Answer: We have modified the Table 1 according to your suggestion. Please see the following Figure.

Table 1. Tree ring cellulose oxygen isotope data sets used in this study

No.	Sample ID	Location	Period	Tree species	Mean (1951-2000)	Climatic response of tree ring $\delta^{18}\text{O}$	Data source
1	Manali	32°13'N, 77°13'E, 2700 masl, India	1768-2008	<i>Abies pindrow</i>	29.97‰	Regional JJAS PDSI $r=-0.67$	Sano et al., submitted
2	JG	29°38'N, 79°51'E, 3849 masl, India	1641-2008	<i>Cedrus deodara</i>	30.39‰	Regional JJAS PDSI $r=-0.50$	This study
3	Hulma	29°51'N, 81°56'E, 3850 masl, Nepal	1778-2000	<i>Abies spectabilis</i>	25.94‰	Regional JJAS PDSI $r=-0.73$	Sano et al., 2011
4	Ganesh	28°10'N, 85°11'E, 3550 masl, Nepal	1801-2000	<i>Abies spectabilis</i>	23.01‰	Regional JJAS PDSI $r=-0.55$	This study
5	Wache	27°59'N, 90°00'E, 3500 masl, Bhutan	1743-2011	<i>Larix griffithii</i>	19.38‰	Regional JJAS PDSI $r=-0.59$	Sano et al., 2013

- In Fig 1 and Table 2 the chronologies from previous studies have a different name. Bhutan in -Table 2 and Wache in Fig 1.

Answer: We have modified the Table 2 according to your suggestion. Please see the following Table 2.

Table 2: Correlation coefficients between the tree ring $\delta^{18}\text{O}$ records from different sampling locations.

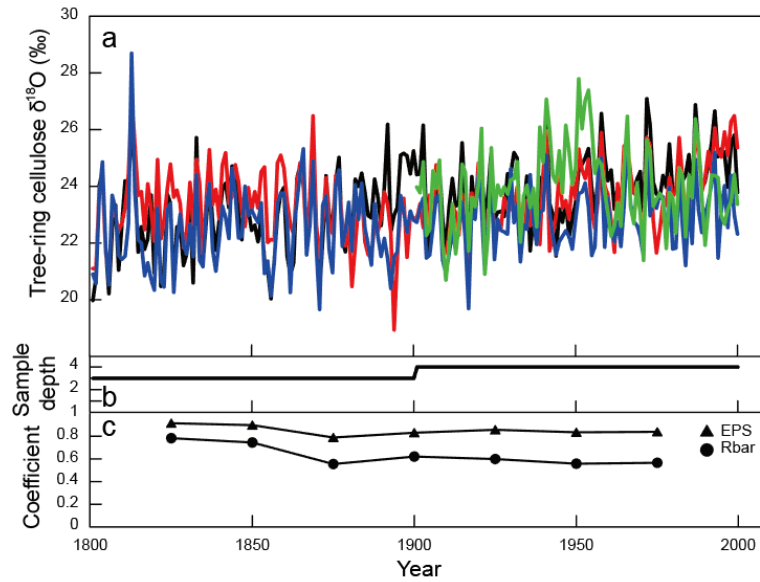
<i>r</i> -annual	Manali	JG	Hulma	Ganesh
JG	0.50*			
Hulma	0.52*	0.51*		
Ganesh	0.47*	0.66*	0.61*	
Wache	0.23*	0.26*	0.37*	0.52*

<i>r</i> -multi-decadal	Manali	JG	Hulma	Ganesh
JG	0.36*			
Hulma	0.37*	0.64*		
Ganesh	-0.03	0.94*	0.66*	
Wache	0.11	0.39*	0.38*	0.70*

* $p<0.01$

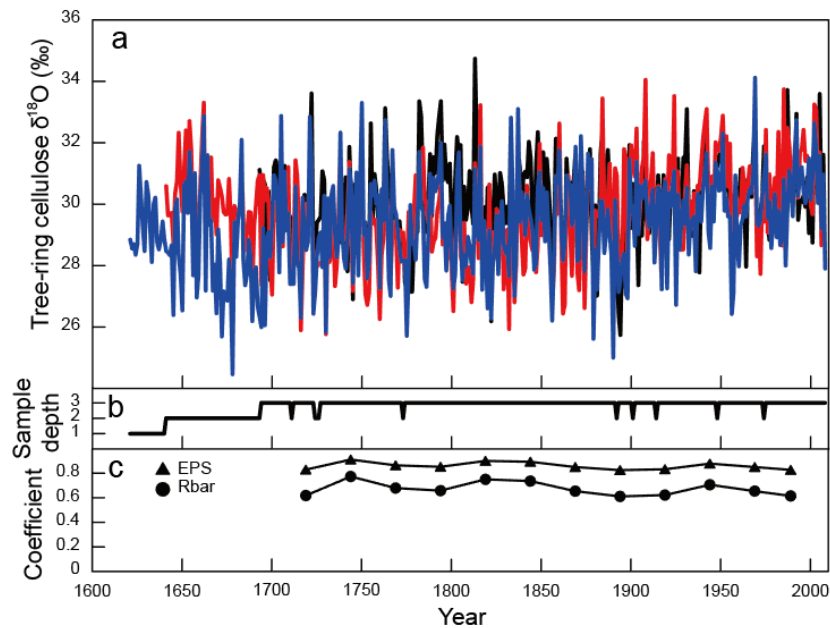
- In Fig 2 the triangle and circle symbols have no legend.

Answer: We have modified the Figure according to your suggestion. Please see the following Figure.



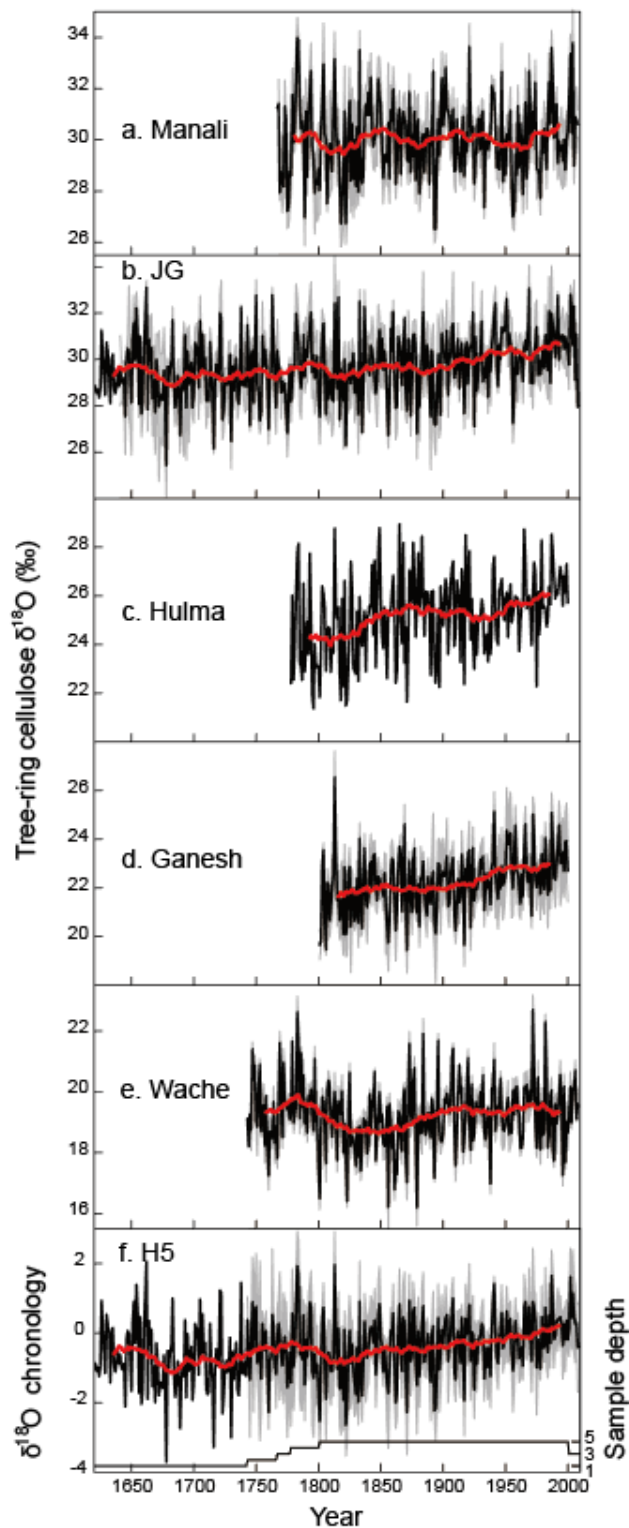
- In Fig 3 the triangle and circle symbols legend is too big. This can be reduced to only the symbols without the line (same should be applied to Fig 2).

Answer: We have modified the Figure according to your suggestion. Please see the following Figure.



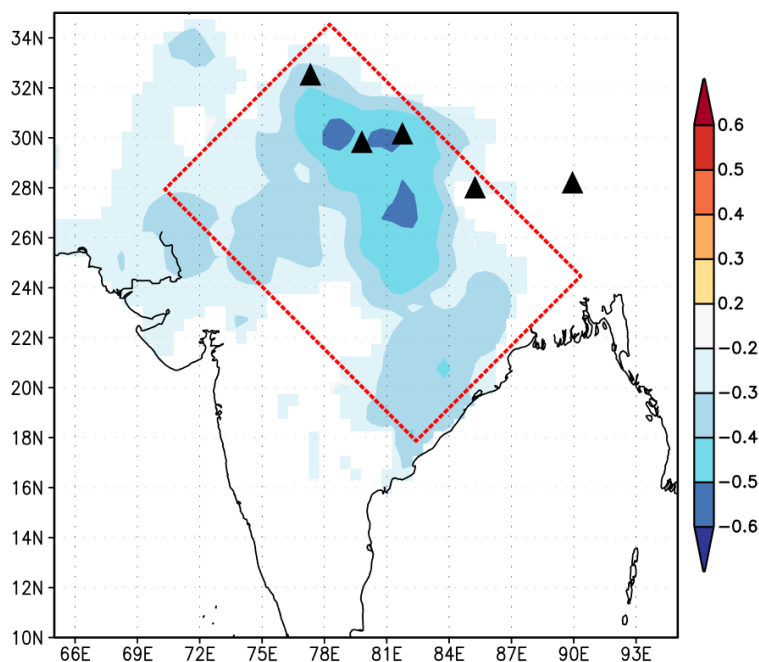
- In Fig 4, the sample depth (number) should be added in a graph below the composite time-series since the number of averaged trees over time is not the same (prior to 1740 and after 2000).

Answer: We have added the sample depth in the Figure according to your suggestion. Please see the following Figure.



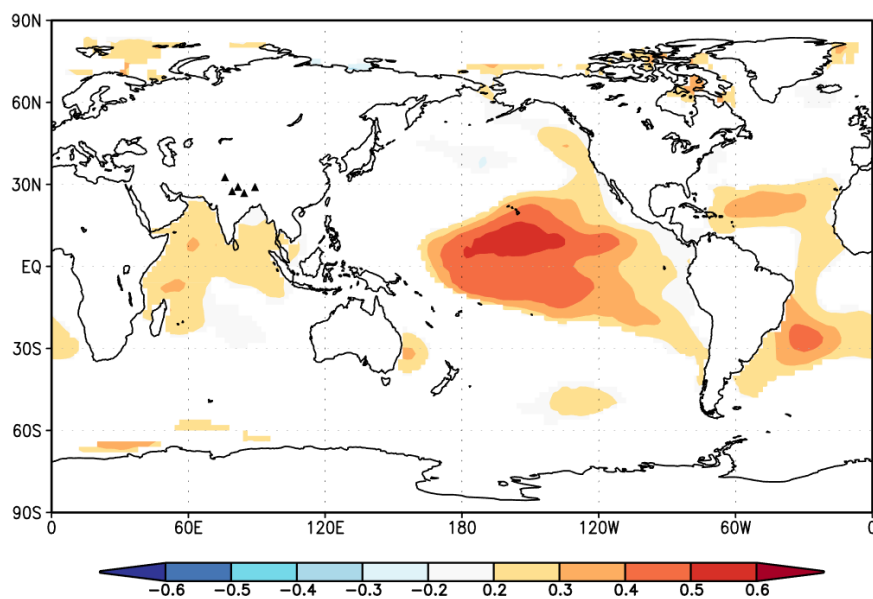
- In Fig 5, add the location of all the sites to help visualize the strength of the field correlations.

Answer: We have modified the Figure according to your suggestion. Please see the following Figure.



- In Fig 8, add the location of the 18O chronologies for spatial reference of the SST correlations.

Answer: We have modified the Figure according to your suggestion. Please see the following Figure.



-Page 8 line 1, a word or punctuation is missing after the parenthesis (eastern-Pacific el Nino).

Answer: We have modified the related part according to your suggestion. Please see the revised part. “Most proxy-based ENSO reconstructions focused on canonical El Niño events (eastern-Pacific El Niño) that are characterized by unusually warm sea surface temperatures (SST) in the eastern equatorial Pacific (Gergis and Fowler, 2009; Li et al., 2011; McGregor et al., 2010)”.